Steel and Composite Structures, *Vol. 15, No. 5 (2013) 519-538*
DOI: http://dx.doi.org/10.12989/scs.2013.15.5.519

An efficient genetic algorithm for the design optimization of cold-formed steel portal frame buildings

D.T. Phan [1], J.B.P. Lim [*2], T.T. Tanyimboh [3] and W. Sha [2]

[1] *Department of Civil Engineering, Universiti Tunku Abdul Rahman, Kuala Lumpur, 53300, Malaysia*
[2] *School of Planning, Architecture and Civil Engineering, Queen's University Belfast, David Keir Building, Belfast, BT9 5AG, UK*
[3] *Department of Civil and Environmental Engineering, University of Strathclyde, John Anderson Building, Glasgow, G4 0NG, UK*

(*Received May 28, 2012, Revised July 18, 2013, Accepted August 05, 2013*)

Abstract. The design optimization of a cold-formed steel portal frame building is considered in this paper. The proposed genetic algorithm (GA) optimizer considers both topology (i.e., frame spacing and pitch) and cross-sectional sizes of the main structural members as the decision variables. Previous GAs in the literature were characterized by poor convergence, including slow progress, that usually results in excessive computation times and/or frequent failure to achieve an optimal or near-optimal solution. This is the main issue addressed in this paper. In an effort to improve the performance of the conventional GA, a niching strategy is presented that is shown to be an effective means of enhancing the dissimilarity of the solutions in each generation of the GA. Thus, population diversity is maintained and premature convergence is reduced significantly. Through benchmark examples, it is shown that the efficient GA proposed generates optimal solutions more consistently. A parametric study was carried out, and the results included. They show significant variation in the optimal topology in terms of pitch and frame spacing for a range of typical column heights. They also show that the optimized design achieved large savings based on the cost of the main structural elements; the inclusion of knee braces at the eaves yield further savings in cost, that are significant.

Keywords: optimization; cold-formed steel; portal frames; niching; real-coded genetic algorithm

1. Introduction

Cold-formed steel portal frames are an increasingly popular form of construction in Australia and the UK, used for low-rise commercial, light industrial and agricultural buildings. For frames of modest spans of up to 20 m, this type of construction has been shown to be a viable alternative to conventional hot-rolled steel portal frames (Lim and Nethercot 2004).

The design optimization of portal frames, in particular for hot-rolled steel standard sections, has attracted the attention of many researchers in recent years (Saka 2003, Hernández *et al*. 2005, Issa and Mohammad 2010). In these studies, a fixed frame spacing and pitch was assumed, with the binary coded genetic algorithm (GA) designating hot-rolled steel sections as discrete design variables; the hot-rolled steel sections were chosen from a discrete set of commercially available

*Corresponding author, Ph.D., E-mail: j.lim@qub.ac.uk

http://www.techno-press.org/?journal=scs&subpage=8 ISSN: 1229-9367 (Print), 1598-6233 (Online)

standard steel sections.

However, in the optimum design of cold-formed steel portal frames, there is a scope to vary the roof pitch and frame spacing, in conjunction with selecting the most appropriate cross sections for the members. This is because cold-formed steel sections are lighter than hot-rolled steel sections, so structural members can be bolted and erected on site by semi-skilled workers, without the need for an onsite crane; consequently, erection costs are much lower than in hot-rolled steel portal frames. A design optimization described by Phan *et al*. (2013) demonstrated that topology can have a significant effect on minimizing the cost of the primary members per meter length of the building.

In engineering optimization, there can be a large number of complex (i.e., multi-modal and non-continuous) objective functions with implicit constraints that require the global optimum solution to be determined. In such problems, the traditional methods of mathematical programming that require the gradients of the objective functions and associated constraints, are not guaranteed to achieve the global or near-global optimum solution due to the possible existence of local minima. As an alternative, GAs that simulate natural phenomena, such as survival of the fittest and adaptation, have been widely used in many fields including in the design optimization of steel structures (Pezeshk *et al*. 2000, Hasançebi *et al*. 2010).

Although GAs have been applied to many engineering problems, the main disadvantage of GAs is that they often suffer premature convergence and weak exploitation capabilities (Goldberg and Richardson 1987). Premature convergence, which often leads to a non-optimal solution or a local optimum solution, can occur because of loss of diversity in the population of candidate solutions. This loss of population diversity is due to the tendency of the selection operator in GAs to favour the better solutions, when choosing solutions to take part in crossover, to create the next generation of solutions. In later generations, the best solutions will therefore dominate the population in the evolutionary processes.

For instance, in the design optimization of hot-rolled steel portal frames having haunch rafters, Saka (2003) used binary-coded GA to minimize the weight of the frame, with four discrete variables, namely, cross-section sizes of column and rafter, and length and depth of the haunch. The optimization process determined the most appropriate sections for members from the list of standard hot-rolled sections and optimum haunch sizes. Saka observed that with a population of 50 and 75 generations the optimum solution occurred in 8 out of 10 runs. Also, using a binary-coded GA to optimize a hot-rolled steel multi-storey frame, Toporov and Mahfouz (2001) modified the conventional GA to improve the performance of the genetic search by maintaining a population containing good individuals for mating. Through two benchmark examples, namely, a five-bay five-storey and a four-bay ten-storey framework, five runs of the GA produced different results. This inability to achieve the optimum solution consistently using binary coded GA has also been addressed in Kameshki and Saka (2001). The same drawback was found in Phan *et al*. (2013), while optimizing the topology of the cold-formed steel portal frame buildings using a real-coded genetic algorithm (RC-GA); it was observed that only 6 out of 10 runs generated the best solution found.

In an effort to enhance the searching performance and accelerate the convergence speed of the GA, a modification of the distributed GA (DGA) was suggested that uses a number of variable mutation schemes to increase the diversity of the population in the earlier stages (Issa and Mohammad 2010). In addition, the niching techniques suggested have been successfully applied to GA in determining the optimum solution of many complicated mathematical functions with multiple constraints (Deb and Goldberg 1989, Deb 2001, Yu and Sugathan 2010).

In this paper, a niching strategy as proposed in Deb (2001) is incorporated into the RC-GA to improve the exploration of the solution space to help achieve the optimum solutions, which are building topology as the continuous variables and section sizes as the discrete variables. The proposed optimization method, to be referred to as real-coded niching GA (RC-NGA), maintains the diversity of the population, thereby increasing the probability of achieving the optimum solution, by the preferential retention of candidate solutions from regions that are under-represented whilst simultaneously eliminating some of the candidate solutions from regions that are overcrowded based on the presumption that candidate solutions in the same neighbourhood would tend to be similar.

The results of RC-NGA, in terms of cost of the primary members per square meter of floor plan, are shown to be identical to the benchmark examples presented in Phan *et al*. (2013). It is shown that the effectiveness in achieving the optimum solution increased significantly in terms of the reliability of the solutions, robustness and computational efficiency. RC-NGA is then used for the purpose of a parametric study that investigates the effect of topology on different sizes of portal frame. The Australian code of practice is used for demonstration purposes, although any design codes can also be applied. The Australian code is used because there is less snow in many regions in Australia, so larger spans can be achieved.

2. Design optimization of the cold-formed steel portal frames

2.1 The details of portal frame building

In this paper, the design optimisation of two types of portal frame is considered: Type 1 without knee braces (Fig. 1(a)) and Type 2 with knee braces (Fig. 1(b)). The joints between members are formed through brackets bolted to the webs of the channel-sections being connected; matching swages rolled into both the brackets and webs of the channel-sections interlock under load forming a joint that can be considered to function as rigid (Kirk 1986). The geometry parameters are as follows: span of frame L_f, height to eaves h_f, pitch of frame θ_f, and frame spacing b_f (Fig. 2). For the case of portal frames having knee braces at the eaves, the position of the knee braces is fixed relative to the height to the eaves, h_f as shown in Fig. 1(b)).

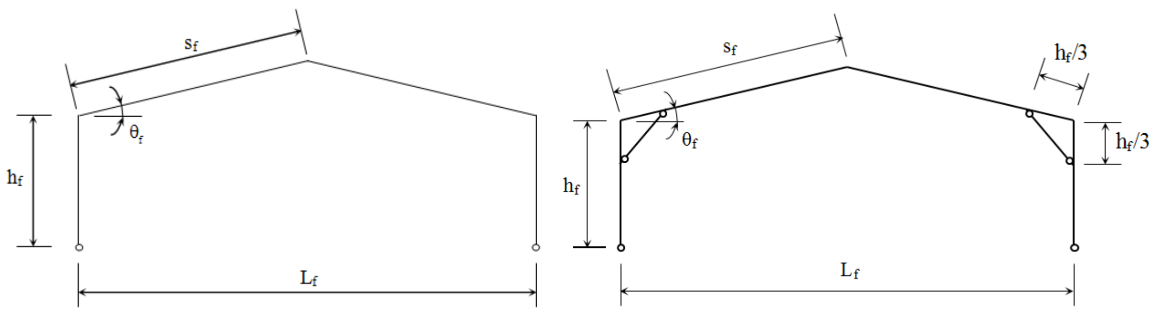

(a) Type 1
Rigid-jointed frame

(b) Type 2
Rigid-jointed frame having knee braces at the eaves

Fig. 1 Geometries of cold-formed steel portal frames

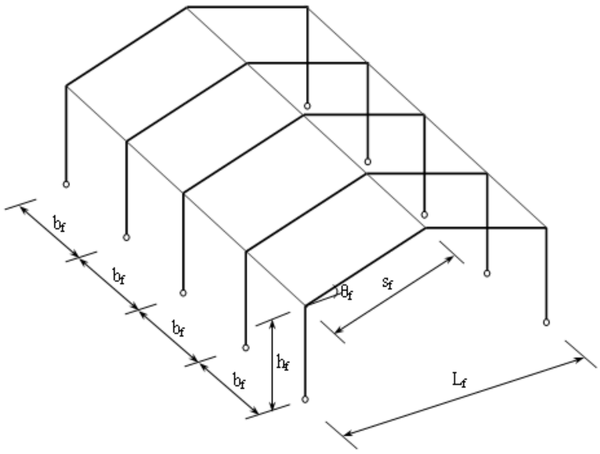

Fig. 2 Parameters of topography of steel portal frame building (purlins, side rails and cladding not shown)

For a specific portal frame building, in which the span of the frame and column height are given, the remaining parameters, i.e., the pitch of the frame and frame spacing, can be varied as topology variables in order to investigate their effect on the unit cost of the building. In this research, the pitch θ_f varies in the range of [5°, 45°]; frame spacing b_f varies in the range of [2 m, 8 m]. Apart from these, the section sizes of members are the other discrete decision variables that are also optimized. As can be seen from Table 1, the most appropriate cross-section sizes are selected from a list of 20 available channel-sections in Australia. These channel-sections can either be used singly or back-to-back (Fig. 3), resulting in 40 combinations. The swages on the web of the channel-sections obviously improve the load carrying capacity of the members. However, for simplifying the checking procedure and obtaining a conservative design, it should be noted that the section properties and member checks are based on plane channel-sections and therefore ignore the benefit of the swages.

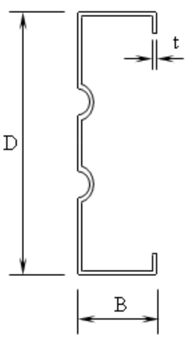

(a) Single channel-section (C)

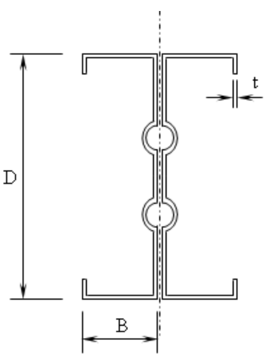

(b) Back-to-back channel-section (BBC)

Fig. 3 Details of cold-formed steel channel-section

It is assumed that the columns bases are pinned. Also, it is assumed that the purlins and side rails are positioned within the web of the members and are spaced sufficiently close to each other to prevent out-of-plane buckling from being the critical failure mechanism.

In many practical cases, the panel zone strength has a great effect on the inelastic response of a moment connection. For strong-axis connections, the panel zone is a portion of the column web, but for weak-axis connections, the panel zone is a portion of the column flanges. Thus, in general, the panel zone strength of weak-axis connections is much higher than that of strong-axis connections. The panel zone strength ratio (V_y / V_{pzMy}) of these weak-axis specimens was 2.35, where V_y is the panel zone yield strength and V_{pzMy} is the panel zone shear force when the connected beam yields.

2.2 Optimization formulation

The objective of the overall design optimization, including the topology and section sizes, is to determine the portal frame building having the minimum cost, whilst satisfying the design requirements. The cost of the main frame, which depends on frame spacing, pitch and cross-section sizes, can be expressed in terms of the cost of the primary members per square metre of the floor area as follows:

$$\text{Minimize } W = \frac{1}{L_f b_f} \sum_{i=1}^{m} w_i l_i \quad (1)$$

where

W	is the cost of main frame per square meter of floor area
w_i	are the cost per unit length of cold-formed steel sections (Table 1)
l_i	are the lengths of cold-formed steel structural members
m	is the number of members.

It should be noted that the frame span L_f appearing in Eq. (1) does not have any effect on the unit cost W, since it is fixed in this paper. However, the unit cost per square meter on building plan can provide practical information for the designers.

2.3 Frame loadings

2.3.1 Permanent and imposed roof loads

The permanent and imposed roof loads according to Australian code (AS/NZS1170-1 2002) that will be applied to the frames are as follows:

Permanent load (G):	0.15 kN/m^2 (purlins, rails, cladding)
	self-weight of the members (see Table 1)
Imposed load (Q):	0.25 kN/m^2

2.3.2 Wind loads

In this paper, wind pressures from wind region *W* in Australia having a regional wind speed V_R of 49.4 m/s are used, based on the Australian code of practice on wind load for the design of buildings (AS/NZS1170-2 2002). According to this code, the basic wind pressure q_u for the ultimate limit state is calculated from a design wind speed V_{des}, which in turn is calculated from the regional wind speed V_R multiplied by factors M_d (wind direction multiplier), $M_{z,cat}$ (terrain/height

Table 1 Dimensions and section properties of cold-formed steel sections

Section	*D* (mm)	*B* (mm)	*t* (mm)	EA($\times 10^2$) (kN)	EI ($\times 10^6$) (kNmm^2)	Weight (kg/m)	Cost (A$/m)
C10010	102	51	1.0	451.0	73.8	1.78	5.58
C10012	102	51	1.2	533.0	88.2	2.10	6.15
C10015	102	51	1.5	656.0	110.7	2.62	6.77
C10019	102	51	1.9	840.5	137.4	3.29	8.37
C15010	152	64	1.0	604.8	225.5	2.32	7.03
C15012	152	64	1.2	717.5	264.5	2.89	7.99
C15015	152	64	1.5	902.0	330.1	3.59	8.46
C15019	152	64	1.9	1148.0	414.1	4.51	10.52
C15024	152	64	2.4	1455.5	520.7	5.70	12.88
C20012	203	76	1.2	922.5	574.0	3.50	8.99
C20015	203	76	1.5	1148.0	723.7	4.49	10.04
C20019	203	76	1.9	1455.5	924.6	5.74	12.56
C20024	203	76	2.4	1845.0	1166.5	7.24	15.29
C25015	254	76	1.5	1312.0	1250.5	5.03	13.66
C25019	254	76	1.9	1660.5	1562.1	6.50	14.43
C25024	254	76	2.4	2091.0	1972.1	8.16	17.82
C30019	300	96	1.9	2070.5	2788.0	7.92	22.76
C30024	300	96	2.4	2583.0	3485.0	10.09	29.52
C30030	300	96	3.0	3280.0	4366.5	12.76	36.25
C35030	350	125	3.0	3915.5	7339.0	15.23	44.74

Table 2 Coefficients of external pressure C_{pe} (AS/NZS1170-2 2002)

Description	Coefficient C_{pe} on face			
	AB	BC	CD	DE
Wind acting on side of frame (*WT*1)	0.7	– 0.3	– 0.3	– 0.3
Wind acting on side of frame (*WT*2)	0.7	– 0.7	– 0.3	– 0.3
Wind acting on end of frame (*WL*1)	– 0.65	– 0.9	– 0.9	– 0.65
Wind acting on end of frame (*WL*2)	– 0.2	0.2	0.2	– 0.2

multiplier), M_s (shielding multiplier), and M_t (topographic multiplier). It is worth noting that $M_{z,cat}$ depends on both the terrain category and the average height of the building. A detailed example of determining the design wind speed and basic wind pressure for a typical portal frame building having span of 20 m, column height of 4 m, and pitch of 10° was presented in Phan *et al*. (2013). In this case, the design wind speed V_{des} is 42.98 m/s and the basic wind pressure q_u is 1.1 kN/m^2.

The design wind pressures acting on each of the four sides of the frame are obtained by multiplying q_u by a coefficient of pressure and other related factors. The coefficient of pressure acting on each face is obtained from a combination of the external pressure coefficient C_{pe} and the internal pressure coefficient C_{pi}. The external pressure coefficients C_{pe} should be calculated for wind acting on the side and on the end. These values are shown in Table 2, calculated based on AS/NZS1170-2 (2002). For buildings of normal permeability, without dominant openings, C_{pi} has a minimum value of – 0.3 for suction, and a maximum value of + 0.2 for pressure.

The eight wind load combinations ($WLC1$ to $WLC8$) for the frame, and their corresponding coefficients for both side wind and end wind, are shown in Table 3. The coefficients of pressures C_{pe} given by $WLC1$ are illustrated in Fig. 4. As can be seen, the frame will be checked for all eight wind load combinations (Table 3) in the design procedure to be described in Section 2.4.

2.3.3 Limit state design

In accordance with the Australian code in AS/NZS1170-0 (2002), the frame will be checked at the ultimate limit state for the following three ultimate load combinations (ULCs)

$$\begin{aligned} ULC1 &= 1.2G + 1.5Q \\ ULC2 &= 1.2G + WLC \\ ULC3 &= 0.9G + WLC \end{aligned} \tag{2}$$

It should be noted that ULC3 is used for the uplift wind load combination.

Table 3 Coefficients of pressure ($C_{pe} + C_{pi}$) corresponding to different wind load cases (AS/NZS1170-2 2002)

Wind load combination	Description	Coefficient on face			
		AB	BC	CD	DE
$WLC1$	Wind on side + internal pressure	0.7 + 0.2	– 0.3 + 0.2	– 0.3 + 0.2	– 0.3 + 0.2
$WLC2$	Wind on side + internal suction	0.7 – 0.3	– 0.3 – 0.3	– 0.3 – 0.3	– 0.3 – 0.3
$WLC3$	Wind on side + internal pressure	0.7 + 0.2	– 0.7 + 0.2	– 0.3 + 0.2	– 0.3 + 0.2
$WLC4$	Wind on side + internal suction	0.7 – 0.3	– 0.7 – 0.3	– 0.3 – 0.3	– 0.3 – 0.3
$WLC5$	Wind on end + internal pressure	– 0.65 + 0.2	– 0.9 + 0.2	– 0.9 + 0.2	– 0.65 + 0.2
$WLC6$	Wind on end + internal suction	– 0.65 – 0.3	– 0.9 – 0.3	– 0.9 – 0.3	– 0.65 – 0.3
$WLC7$	Wind on end + internal pressure	– 0.2 + 0.2	0.2 + 0.2	0.2 + 0.2	– 0.2 + 0.2
$WLC8$	Wind on end + internal suction	– 0.2 – 0.3	0.2 – 0.3	0.2 – 0.3	– 0.2 – 0.3

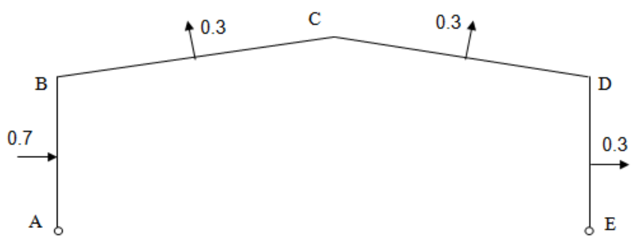

Fig. 4 Coefficients of wind pressure for wind load combination 1 ($WLC1$)

2.4 Frame design

A first-order elastic frame analysis program is used to analyze the portal frame. For each load combination, bending moment, shear force and axial force diagrams for the frame are determined. The frame analysis program is called to analyse each candidate solution from current population in each generation as shown in Fig. 5.

Columns and rafters

In accordance with AS/NZS 4600 (2005), the column and rafters are checked for combined axial compression and bending, distortional buckling, and combined bending and shear. In the case of portal frames having knee braces at eaves, the knee braces are checked for both buckling under compression and tension. The section capacities of lipped channel-sections without swages is calculated on the basis of effective width method (EWM) given in the Chapter 2 and 3 of this code; the effect of swages on the web is neglected to simplify the problem.

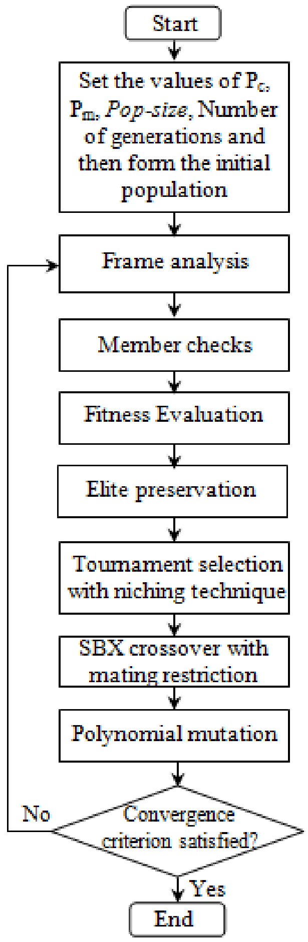

Fig. 5 Flowchart of the real-coded niching genetic algorithm

The combined axial force and bending constraint is

$$\frac{N_k^*}{\phi_c N_s^k} + \frac{M_{xk}^*}{\phi_b M_s^k} \leq 1 \tag{3}$$

where

N_s^k	is the nominal section capacity of member *k* in compression
M_s^k	is the nominal section moment capacity of member *k* about the x-axis
N_k^*	is the design axial compression in member *k*
M_{xk}^*	is the design bending moment in member *k* about x-axis of the effective cross-section
ϕ_c	is the capacity reduction factor for compression
ϕ_b	is the capacity reduction factor for bending

The distortional buckling check is

$$M_{xk}^* \leq \phi_b M_{bx}^k \tag{4}$$

with $M_{bx}^k = Z_c f_c$ and $f_c = M_c / Z_f$

where

M_{xk}^*	is the design bending moment in member k about x-axis of the effective cross-section
ϕ_b	is the capacity reduction factor for bending
M_{bx}^k	is the nominal member moment capacity of member *k*
Z_c	is the effective modulus at a stress f_c in the extreme compression fibre
M_c	is the critical moment
Z_f	is the full unreduced section modulus for the extreme compression fibre

The combined bending and shear check is

$$\frac{M_{xk}^*}{\phi_b M_s^k} + \frac{V_k^*}{\phi_v V_{vk}} \leq 1 \tag{5}$$

where

M_{xk}^*	is the design bending moment in member *k* about *x*-axis of the effective cross-section
M_s^k	is the nominal section moment capacity of member *k* about the *x*-axis
V_k^*	is the design shear force in member *k*
V_{vk}	is the nominal shear capacity of the web of member *k*
ϕ_b	is the capacity reduction factor for bending
ϕ_v	is the capacity reduction factor for shear.

Eaves knee braces

The knee brace is a pin-ended member and is checked for both compression and tension. The compression check is

$$N_{ck}^* \leq \phi_c N_{ck} \tag{6}$$

where

M^*_{ck} is the design compressive axial force of member k
N_{ck} is the nominal member capacity of the member k in compression
ϕ_c is the capacity reduction factor for compression

The tension check is

$$N^*_{tk} \le \phi_t N_{tk} \tag{7}$$

where
N^*_{tk} is the design tensile force of member k
N_{tk} is the nominal section capacity of the member k in tension
ϕ_t is the capacity reduction factor for tension.

3. Real-coded niching genetic algorithm (RC-NGA)

The design optimization considered in this paper contains mixed discrete and continuous decision variables. As demonstrated in Deb (2001), RC-GA is appropriate for this problem, especially as the optimization of the topology of the cold-formed steel portal frame building involves continuous decision variables. The benefit of RC-GA is that genetic operators are directly applied to the design variables without coding and decoding as with binary GAs. In addition, for discrete design variables, a technique that rounds off the results of the simulated binary crossover (SBX) and polynomial mutation that are described later in this section is used.

3.1 The niching strategy in the selection operator

In the proposed RC-NGA, tournament selection with a niching technique is applied. The process is conducted by selecting at random two individuals from the current population, namely $x^{(i)}$ and $x^{(j)}$. The normalized Euclidean distance (Deb 2000) between the two solutions is

$$d_{ij} = \sqrt{\frac{1}{n}\sum_{k=1}^{n}\left(\frac{x_k^{(i)} - x_k^{(j)}}{x_k^u - x_k^l}\right)^2}\ ;\ \ 1 \le i, j \le Pop-size \tag{8}$$

where
d_{ij} is a normalized Euclidean distance between $x_k^{(i)}$ and $x_k^{(j)}$
n is the number of decision variables
Pop-size is the population size in the RC-NGA
$x_k^{(i)}$ and $x_k^{(j)}$ are the corresponding k^{th} decision variable in two vectors $x_k^{(i)}$ and $x_k^{(j)}$.
x_k^u and x_k^l are the upper and lower bounds respectively of the k^{th} decision variable.

If this Euclidean distance is smaller than an empirical user-defined critical distance, these solutions are compared using their fitness function values. Otherwise, they are not compared and another solution $x^{(j)}$is selected at random from the population for comparison. If after a certain number of checks, no solution $x^{(j)}$ is found to satisfy the critical distance, $x^{(i)}$ is selected for the crossover operation. In this way, only solutions in same region (or niche) compete against each other for selection and crossover.

3.2 The real-coded genetic operators

The crossover operator for RC-NGA uses the simulated binary crossover (SBX) formula to apply directly to real variables (Deb and Agrawal 1995). Apart from that, Deb (2001) observed that with the crossover operator applied uniformly to the whole population, some search effort is wasted in the recombination of solutions as their distance is larger than the critical distance. A mating restriction scheme is therefore applied to prevent individuals in different niches from mating each other. Only two individuals that are located within a normalized Euclidean distance (see Eq. (8)) smaller than a predefined distance, or in the same niche, should be allowed to become mating partners. For two solutions satisfying the mating restriction, the SBX operator is as follows

$$\begin{aligned} x_k^{(1,t+1)} &= 0.5\,[(1+\beta)x_k^{(1,t)} + (1-\beta)x_k^{(2,t)}] \\ x_k^{(2,t+1)} &= 0.5\,[(1-\beta)x_k^{(1,t)} + (1+\beta)x_k^{(2,t)}] \end{aligned} \tag{9}$$

where

- β is the probability distribution function for crossover
- $x_k^{(1,t)}$ and $x_k^{(2,t)}$ are the values of the k^{th} decision variable for the parent solutions
- $x_k^{(1,t+1)}$ and $x_k^{(2,t+1)}$ are the values of the k^{th} decision variable of the children created for the next generation.

To ensure the new values of the decision variable remain within the range $[x_k^l, x_k^u]$, where x_k^l and x_k^u are the lower and upper bounds, respectively, the probability distribution for the crossover operator has the form

$$\beta(\eta_c) = \begin{cases} [\alpha u]^{1/(\eta_c+1)} & if \quad u \le 1/\alpha, \\ [1/2 - \alpha u]^{1/(\eta_c+1)} & if \quad 1/\alpha < u \le 1 \end{cases} \tag{10}$$

with

$$\alpha = 2 - \chi^{-(\eta_c+1)}$$

$$\chi = 1 + \frac{2}{x_k^{(2,t)} - x_k^{(1,t)}} \min\left[(x_k^{(1,t)} - x_k^l), (x_k^u - x_k^{(2,t)})\right]; \text{ assuming } x_k^{(1,t)} < x_k^{(2,t)}$$

where

- u is a random number between 0 and 1,
- η_c is the distribution index for crossover; $\eta_c = 1$ herein.

The mutation operator for RC-NGA mutates at random one solution in the population and employs the polynomial mutation formula (Deb 1989, Deb and Gulati 2001)

$$y_k^{(1,t+1)} = x_k^{(1,t+1)} + (x_k^u - x_k^l)\bar{\delta} \tag{11}$$

where

- x_k^u and x_k^l are upper and lower bounds, respectively, of the k^{th} decision variable
- $y_k^{(1,t+1)}$ is a new value obtained from the mutation operator and it replaces $y_k^{(1,t+1)}$.

To ensure that no solution would be created outside the range of x_k^u and x_k^l the parameter $\bar{\delta}(\eta_m)$

has the form (Deb and Gulati 2001)

$$\bar{\delta} = \begin{cases} \left[2u + (1-2u)(1-\delta)^{\eta_m+1}\right]^{1/(\eta_m+1)} - 1 & if \quad u \le 0.5, \\ 1 - \left[2(1-u) + 2(u-0.5)(1-\delta)^{\eta_m+1}\right]^{1/(\eta_m+1)} & if \quad 0.5 < u \le 1 \end{cases} \tag{12}$$

with

$$\delta = \min\left[(x^{(1,t+1)} - x_k^l), (x_k^u - x^{(1,t+1)})\right] / (x_k^u - x_k^l)$$

where

- u is a random number between 0 and 1
- η_m is the distribution index for mutation; $\eta_m = 1$ herein.

The flowchart of the RC-NGA used in this paper is shown in Fig. 5. Constant probabilities are assigned to both crossover and mutation operators. Based on a number of trials, a crossover probability P_c of 0.9 is used throughout in this study. It was observed that premature convergence happens with a low mutation probability. To increase the GA's exploration capacity in the solution space to increase the chance of locating the optimum solution, the mutation probability P_m is tuned empirically to as high as 0.1. The high value of mutating probability used in this paper was also used in Deb and Gulati (2001).

3.3 Fitness function and penalized technique

The ultimate limit state (ULS) described in Section 2.4 is the basis of the design constraints for the optimization problem. A penalty function is used to transform this constrained problem to an unconstrained one. Penalty values are imposed empirically, in proportion to the severity of constraint violation. The fitness function adopted has the form as follows

$$F = W[1 + C] \tag{13}$$

where

- F is the fitness function
- W is the objective function being the cost of frame per unit area
- C is the constraint violation penalty.

The normalized forms of the design constraints or unity-factors given in Eqs. (3)-(7) are processed in GA as follows

$$g_1 = \frac{N_k^*}{\phi_c N_s^k} + \frac{M_{xk}^*}{\phi_b M_s^k} - 1 \le 0 \tag{14a}$$

$$g_2 = \frac{M_{xk}^*}{\phi_b M_b^k} - 1 \le 0 \tag{14b}$$

$$g_3 = \frac{M_{xk}^*}{\phi_b M_s^k} + \frac{V_k^*}{\phi_v V_{vk}} - 1 \le 0 \tag{14c}$$

$$g_4 = \frac{N_{ck}^*}{\phi_c N_{ck}} - 1 \le 0 \tag{14d}$$

$$g_5 = \frac{N_{tk}^*}{\phi_t N_{tk}} - 1 \le 0 \tag{14e}$$

The penalty value is assigned through the maximum level of violation of the unity-factor constraints in Eqs. (14a)-(14e) as follows

$$g = \max[g_1, g_2, g_3, g_4, g_5] \tag{15}$$

Through a numbers of trials, it is observed that two levels of constraint violation penalties with the magnitudes as shown in Eq. (16) are suitable

$$C = \begin{cases} 0 & if \quad g \le 0 \\ g & if \quad 0 < g \le 0.5 \\ 10g & if \quad g > 0.5 \end{cases} \tag{16}$$

The proposed optimization procedure aims to minimize the value of the fitness function F (Eq. (13)). This is achieved by minimizing the cost W and reducing the penalty *C* to zero. The procedure involves RC-NGA and frame analysis modules (Fig. 5). In this optimization process, the evaluation process computes the fitness function values using the objective function (Eq. (1)) along with the corresponding penalty values defined in Eq. (16). Better (i.e., cheaper) solutions will yield smaller fitness values, and consequently are selected preferentially by the tournament selection operator. The criterion for terminating the program is a predefined total number of function evaluations or generations.

4. Benchmark examples

4.1 Portal frame without knee braces (*Type 1*)

The design optimization for Frame Type 1 is considered using RC-NGA. The frame has a span of 20 m and column height of 4 m. This benchmark example was described in Phan *et al*. (2013) and solved using RC-GA. The design optimization that accounts for the effect of both the pitch and frame spacing is conducted with the GA parameters and operators described in the Section 3. This problem has four decision variables, *viz*. pitch and frame spacing processed as continuous variables, whilst cross-section sizes of the columns and rafters being the discrete ones.

For the proposed optimization algorithm, the initial population is established randomly. Through a number of trials with different sizes, the size of population is chosen as 40, in the design example considered. Since the normalized Euclidean distance in Eq. (8) has a range from 0 to 1, it is found empirically that a suitable value of d_{ij} is 0.3, for which tournament selection and crossover operators worked effectively in this study, relating to the selected population size. Crossover probability of 0.9 and mutating probability of 0.1 are used for implementing genetic operators in RC-NGA. Due to the random aspect of the proposed algorithm, the design of frame Type 1 is optimized ten times with different seed values to check for the consistency of the optimum result obtained from every optimization algorithm, namely, RC-NGA and RC-GA. The maximum number of generations was empirically selected as 250 to terminate the program.

It was observed that the RC-NGA, with a population size of 40, produced the same optimum solution in 8 out of 10 runs. The optimization process converged to the optimum solution within the predefined number of generations. The results obtained from 8 runs generating the same solution showed that the most appropriate cross-section size for both the columns and rafters is BBC25024; the optimum pitch is 21°, the optimum bay spacing is 3 m, and the unit cost is A$ 17.75/m^2. As expected, these results obtained were the same as the result generated from the RC-GA in Phan *et al*. (2013). The design constraint for the combined actions of axial compression and bending on rafter was critical, i.e., $g_1 = 0$, with ULC3 load combination. The CPU time for RC-NGA was 1.5 hours for a machine having a processor speed of 2.0 GHz, and memory of 2.0 GB. It is interesting to observe that the other 2 runs generated the frame weight only 5.2% higher cost than the optimum solution, in which the same optimum cross-section size and pitch was obtained, whilst frame spacing was slightly smaller. This clearly showed that the proposed optimization algorithm generated the near-global optimum solution if not global one.

It should be noted that with the same population size of 40, the authors also optimized this design using the RC-GA within 250 generations. The optimization procedure following the GA flowchart as shown in Fig. 5 is applied; however, conventional selection and crossover operators are applied. Conveniently, the RC-NGA will be converted to RC-GA when the niching value is set to unity. It is observed that the best result obtained after ten runs has a unit cost A$ 21.55/m^2, which is 24% higher than the optimum cost obtained from RC-NGA. Browsing the unity factors of constraints, all results are slack, in which the maximum unity factor for the combined actions of axial compression and bending on rafter was critical, i.e., $g_1 = -0.2$, with ULC3 load combination.

The individuals' distribution in the population through the evolutionary process, which generated the best solution after 10 runs, is typically displayed in Fig. 6 for RC-NGA and Fig. 7 for RC-GA. Three parameters, namely, maximum, mean, and minimum costs, are chosen to show the distribution of those individuals in the population. As can be seen in Fig. 6, the diversity of the population was maintained through the mean cost is around half way between maximum and minimum costs. On the other hand, as can be seen in Fig. 7, the diversity of the population declined considerably; the better fitness solutions dominated the population after 100 generations, so the mean value obtained is rather close to the minimum weight. It explained the weak capacity of RC-GA in searching for the optimum solution with a small population size.

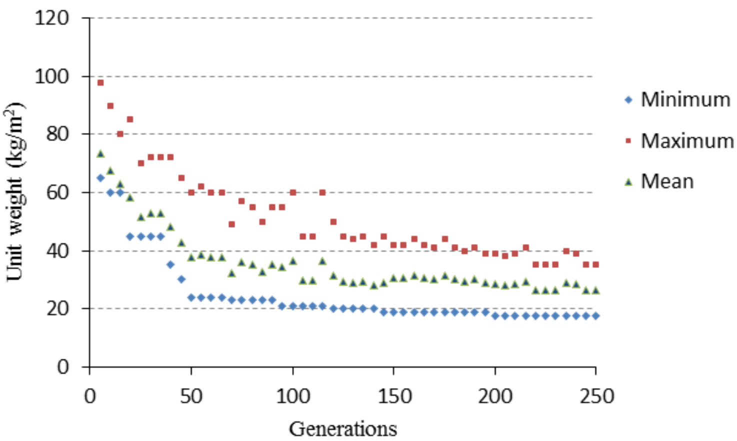

Fig. 6 Convergence progress of RC-NGA for Frame Type 1

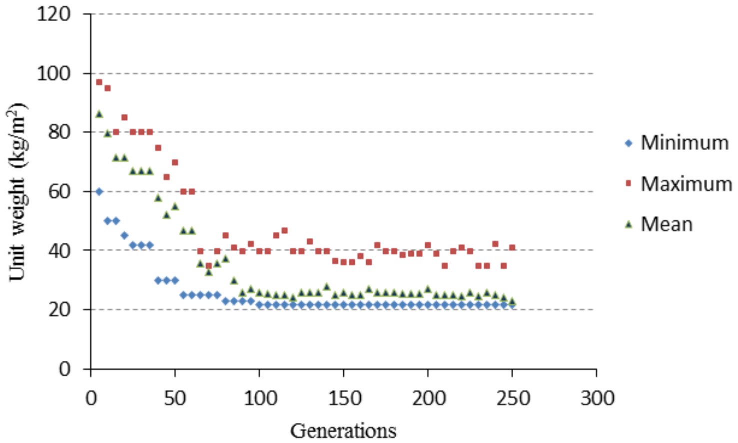

Fig. 7 Convergence progress of RC-GA for Frame Type 1

This showed that the capacity of RC-GA for searching the optimum solution using a small population size is not effective. As observed in the previous research (Phan *et al*. 2013), the suitable population size for RC-GA was 120 to reach a better optimum solution. It was observed that only 5 out of 10 runs, with population size of 120, generated the same optimum solution. Comparing the time for solving the problem, RC-NGA generates the optimum results three times more efficiently than RC-GA.

4.2 Portal frame with knee braces (*Type 2*)

The optimal design of a portal frame with knee braces at eaves (Type 2), having the same span and column height as in Frame Type 1, is considered in this section. There are five design decision variables in this problem: pitch and frame spacing were considered as continuous variables, whilst the column, rafter and knee brace cross-sections were considered as discrete variables. This optimization problem is more complicated than the previous example as there are more design variables and the solution space is larger. The population size was therefore set as 50 and a number of generations of 250 is used to terminate the RC-NGA program. The other genetic parameters, namely, crossover probability of 0.9, mutation probability of 0.1, and niching distance of 0.25 are used for the evolutionary process, as shown in Fig. 5.

Table 4 Optimum solution for Frame Type 2 with variable topography (Phan *et al*. 2013)

Member type	Cold-formed steel sections	g_1	g_2	g_3	g_4	g_5	θ_f	b_f (m)	W (A\$/m^2)
Column	BBC 25024	– 0.01	– 0.03	– 0.09	– 1.00	– 1.00			
Rafter	BBC 25024	0	– 0.01	– 0.07	– 1.00	– 1.00	17.5°	4.0	13.5
Knee brace	C 20015	– 1.00	– 1.00	– 1.00	– 0.02	– 0.38			

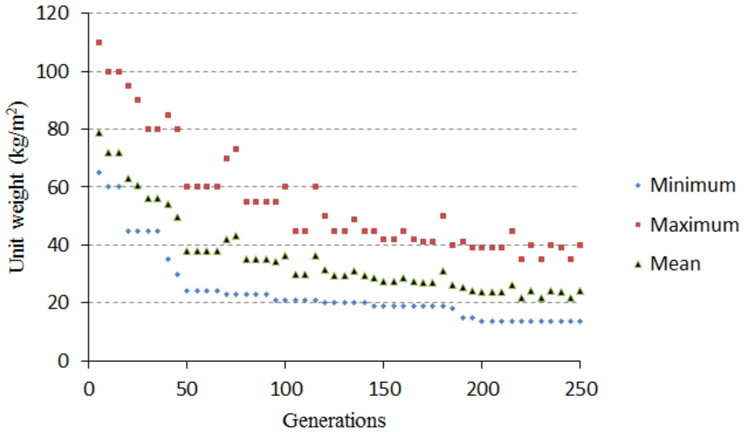

Fig. 8 Convergence progress of RC-NGA for Frame Type 2

With a population size of 50, it was observed that RC-NGA generated the best-known optimum solution in 7 out of 10 runs. The progress of RC-NGA converging to the best optimum solution is shown in Fig. 8. As can be seen, the optimum unit cost obtained is A$ 13.5/m^2 with corresponding parameters as shown in Table 4, which is the same as those results shown in Phan *et al*. (2013). It is interesting to note that the knee braces at the eaves lead to a larger frame spacing being achieved, which makes the unit cost of the Frame Type 2 lower than the cost of Frame Type 1 by 24%. The knee braces also result in the optimum pitch reducing by around 3°, compared with the optimum pitch of the same frame without knee braces. The combined actions of bending moment and axial compression on the rafter is active ($g_1 = 0$) in the case of load combination ULC3.

Similar to the case of the optimization of Frame Type 2, the niching strategy effectively maintained the diversity of the population (see Fig. 8), which can achieve an optimum solution with a small population size. As compared to the RC-GA routine, launched by setting the niching value of unity, it is observed that the procedure converged prematurely at a local optimum solution in all ten runs with the same population size of 50. To improve the performance of the RC-GA, the necessary population size was found as 120 within 250 generations. This enabled 4 runs out of 10 to converge to the lowest cost solution, as found in this work.

It was observed that the computational time for solving the optimization problem using RC-NGA was 2.4 hours using a machine having a processor of 2.0 GHz and memory of 2.0 GB. The improved efficiency of RC-NGA over RC-GA is due to the fact that the diversity of population has been maintained in RC-NGA by niching. Also, the mating restriction increased the exploitation capacity of the algorithm in the local areas. This distinct characteristic is the reason for the greater effectiveness of the smaller population being used.

5. Parametric study

It has been shown that RC-NGA can generate (near) global optimum solutions with a higher consistency and in a reasonable computation time compared with RC-GA. In this section, RC-NGA is therefore used for the purpose of a parametric study on the effect of the pitch and frame spacing on Frames Types 1 and 2. The frames considered all have a span of 20 m. Four typical column heights, as commonly used for cold-formed steel portal frame buildings, are considered: 3 m, 4 m, 5 m, and 6 m. The parameters used in the RC-NGA are as follows: population size of 50, crossover probability of 0.9, mutating probability of 0.1, and niching distance of 0.25. These frames are optimized ten times with different seed values due to the random aspect of the optimal problem. The best results obtained after ten optimization runs are shown in Tables 5, 6 and 7.

Table 5 shows the optimum cross-section sizes of structural members and corresponding unit costs for Frame Type 1 and Frame Type 2 having a small column height of 3 m, with a typical topology (i.e., a frame spacing of 4 m and pitch of 10°). As can be seen, for such portal frame buildings, taking into account the optimum topology, the cost per unit plan area of the building shows the largest savings, for instance 39% for Frame Type 1 (Table 6) and 47% for Frame Type 2 (Table 7), compared with those results shown in Table 5.

As can be seen from Table 6 and Table 7, there is a reducing trend of the optimum frame spacing and pitch when the column height increases from 3 m to 6 m. This is because reducing frame spacing will lead to lower loadings being subjected to the frame. The section sizes of members are therefore smaller/cheaper. It should be noted that the wind load is in proportion to the apex height of the building. This is the reason why the roof pitch achieved a small angle in the case of high column, whilst the large pitch in portal frame gives a better structural performance in the case of small column height.

For the frame without knee braces at eaves, it is interesting to see that the optimum cross-section sizes with the back-to-back channel section BBC25024 are the most appropriate sizes for the four cases of the column heights corresponding to the optimum pitch and frame spacing (Table 6). In addition, the use of knee braces at the eaves results in the optimum pitches being smaller to reduce the length of rafters; the frame spacings, larger than in the case of Frame Type 1, are observed to reduce the unit cost per area on the plan of building. These factors made

Table 5 Optimum section sizes for portal frame with column height of 3 m ($\theta_f = 10°$ and $b_f = 4$ m)

Column height	Members	Frame Type 1	Frame Type 2	Cost (A$/m^2)	
				Frame Type 1	Frame Type 2
3 m	Columns	BBC30030	BBC30024	23.8	23.3
	Rafters	BBC30030	BBC30030		
	Knees	N/A	C15019		

Table 6 Optimum designs for Frame Type 1 as function of column height

Column height	Optimum pitch	Optimum frame spacing (m)	Cost (A$/m^2)
3 m	23°	3.4	14.5
4 m	21°	3.0	17.8
5 m	18°	2.6	21.1
6 m	14°	2.3	25.3

Table 7 Optimum designs for Frame Type 2 as function of column height

Column height	Optimum pitch and frame spacing	Members	Section sizes	Cost (A\$/m^2)	Reduction over Frame Type 1 (%)
3 m	θ_f = 20.5° b_f = 5.0 m	Columns Rafters Knees	C35030 C35030 C15015	12.4	14.5%
4 m	θ_f = 17.5° b_f = 4.0 m	Columns Rafters Knees	BBC25024 BBC25024 C20015	13.5	24.2%
5 m	θ_f = 12° b_f = 3.3 m	Columns Rafters Knees	BBC25024 BBC25024 BBC10015	17.3	18.0%
6 m	θ_f = 10° b_f = 2.6 m	Columns Rafters Knees	BBC25024 BBC25019 C20019	21.3	15.8%

the unit costs of Frame Type 2 lower than Frame Type 1 by up to 24%.

It was observed that all frames shown in this parametric study are optimal design with the critical design constraint for combined axial force and bending moment reaching the upper bounds. The optimum solutions converged within the predefined generations. The consistency of achieving the same optimum solution for all designs above is around 8 out of 10 runs. The time for solving is around 2.4 hours using a machine having a processor of 2.0 GHz and memory of 2.0 GB.

6. Conclusions

The RC-NGA was developed to minimize the cost of the primary members per square meter of floor plan for cold-formed steel portal frame buildings. The consistency of the optimum solution being obtained has been improved, conducted with a medium population size and within a more reasonable computational time. It was shown the diversity in the population has been maintained, so that the probability of achieving the optimum result increased effectively.

For each building, the optimization program aims to determine the optimum topology and the most suitable cross-sections for the members. The frame design obtained from the program can be considered as the most economical design in each case, since the critical design constraint in all examples becomes active. The computational efficiency and robustness of the algorithm has also been demonstrated. The length of computational time for solving the optimization problem was therefore reduced by more than four times in comparison with RC-GA.

A parametric study on a building having a span of 20 m, with four different column heights, shows that the optimum pitch reduces as the column height increases. As expected, the knee brace at the eaves results in larger frame spacing. Although the cost is calculated based on material used for the main frames, the reduction is very remarkable when the optimum topology is reached. For example, for a portal frame having a column height of 3 m and span of 20 m, the optimum topology results in savings of 39% for the frame without knee braces at eaves, and 47% for the frame having knee braces at the eaves, compared with the typical topology of 4 m for the frame spacing and 10° for the pitch.

Acknowledgements

The financial support from the Queen's University Belfast is gratefully acknowledged.

References

Autralian/New Zealand Standard™ (2002), AS/NZS1170-0, *Structural Design Actions – Part 0*: *General principles*, Sydney, Standards Australia.

Autralian/New Zealand Standard™ (2002), AS/NZS1170-1, *Structural Design Actions – Part 1*: *Permanent*, *imposed and other actions*, Sydney, Standards Australia.

Autralian/New Zealand Standard™ (2002), AS/NZS1170-2, *Structural Design Actions – Part 2*: *Wind actions*, Sydney, Standards Australia.

Autralian/New Zealand Standard™ (2005), AS/NZS4600:2005, *Cold-formed Steel Structures*. Sydney, Standards Australia.

Deb, K. (2000), "An efficient constraint handling method for genetic algorithms", *Comput*. *Method*. *Appl*. *Mech*., **186**(2-4), 311-338.

Deb, K. (2001), *Multi-Objective Optimization Using Evolutionary Algorithms*, Chichester: John Wiley and Sons, Inc.

Deb, K. (1997), "Mechanical component design using genetic algorithms", (*In*: *Dasgupta*, *D. and Michalewicz*, *Z. eds*)., Evolutionary Algorithms in Engineering Applications, New York, Springer, 495-512.

Deb, K. and Agrawal, R.B. (1995), "Simulated binary crossover for continuous space", *Complex Systems*, **9**(2), 115-148.

Deb, K. and Goldberg, D.E. (1989), "An investigation of niche and species formation in genetic function optimization", (*In*: *Schaffer*, *J.D. ed*.), *Proceedings of the 3rd International Conference on Genetic Algorithms*, San mateo, Morgan Kauffman, 42-50.

Deb, K. and Gulati, S. (2001), "Design of truss-structures for minimum weight using genetic algorithms", *Finite Elem*. *Anal*. *Des*., **37**(5), 447-465.

Goldberg, D.E. (1989), *Genetic Algorithms in Search*, *Optimization and Machine Learning*, Addison-Wesley Publishing Company, New York, USA.

Goldberg, D.E. and Richardson, J. (1987), "Genetic algorithms with sharing for multimodal function optimization", *Proceedings of the 2nd International Conference on Genetic Algorithms*, L. Erlbaun Associates, 41-49.

Hasançebi, O., Çasbaş, S., Doğan, E., Erdal, F. and Saka, M.P. (2010), "Comparison of non-deterministic search technique in the optimum design of the real size steel frame", *Comput*. *Struct*., **88**(17-18), 1033-1048.

Hernández, S., Fontán, A.N., Perezzán, J.C. and Loscos, P. (2005), "Design optimization of steel portal frames", *Adv*. *Eng*. *Softw*., **36**(9), 626-633

Issa, H.K. and Mohammad, F.A. (2010), "Effect of mutation schemes on convergence to optimum design of steel frames", *J*. *Constr*. *Steel Res*., **66**(7), 954-961.

Kameshki, E. and Saka, M.P. (2001), "Optimum design of nonlinear steel frames with semi-rigid connections using a genetic algorithm", *Comput*. *Struct*., **79**(17), 1593-1604.

Kirk, P. (1986), "Design of a cold-formed section portal frame building system", (*In*: *Yu*, *W.W. and Senne J.H. eds*.), *Proceedings of the 8th International Specialty Conference on Cold-formed Steel Structures*, University of Missouri-Rolla, St. Louis, Missouri, November, 295-310.

Lim, J.B.P. and Nethercot, D.A. (2004), "Finite element idealization of a cold-formed steel portal frame", *J. Struct*. *Eng*. *ASCE*, **130**(1), 78-94.

Miller, B.L. and Shaw, M.J. (1996), "Genetic algorithms with dynamic niche sharing for multimodal function optimization", *Proceedings of the IEEE International Conference on Evolutionary Computation*, Nagoya, Japan, February, 786-791.

Pezeshk, S., Camp, C. and Chen, D. (2000), "Design of nonlinear framed structures using genetic optimization", *J. Struct*. *Eng*. *ASCE*, **126**(3), 382-388.

Phan, D.T., Lim, J.B.P., Sha, W., Siew, C., Tanyimboh, T., Issa, H. and Mohammad, F. (2013), "Design optimization of cold-formed steel portal frames taking into account the effect of topography", *Eng*. *Optimiz*., **86**, 74-84.

Saka, M.P. (2003), "Optimum design of pitched roof steel frames with haunched rafters by genetic algorithm", *Comput*. *Struct*., **81**(18-19), 1967-1978.

Toropov, V.V. and Mahfouz, S.Y. (2001), "Design optimization of structural steelwork using genetic algorithm, FEM and a system of design rules", *Eng*. *Comput*., **18**(3/4), 437-459.

Yu, E.L. and Sugathan, P.N. (2010), "Ensemble of niching algorithms", *Inform*. *Sci*., **180**(15), 2815-2833.

DL